ELSEVIER

Physica B 221 (1996) 430–436

PHYSICA B

Thermal vibration amplitudes and structure of Sb on Si(0 0 1) by X-ray standing waves

Y. Qian[a,b,*], P.F. Lyman[b], Tienlin Lee[b], M.J. Bedzyk[a,b]

[a] *Materials Science Division, Argonne National Laboratory, Bldg. 223, C202, Argonne, IL 60439, USA*
[b] *Department of Materials Science and Engineering and Materials Research Center, Northwestern University, Evanston, IL 60208, USA*

Abstract

X-ray standing waves generated by dynamical Bragg diffraction were used as an element-specific structural probe for investigating Sb adsorption on Si(0 0 1). These high-resolution measurements of the Si(0 0 1)/Sb-(1 × 2) surface reveal important quantitative structural information regarding the dimerized surface structures, such as Sb ad-dimer height, Sb dimer bond length, Sb thermal vibration amplitude, and inward contraction of the Si surface.

1. Introduction

A thorough understanding of the atomic bonding, surface reconstruction, and surface dynamics of group V metals on Si(0 0 1) has been of continuing interest and the subject of many recent experimental and theoretical studies. Technologically, this is motivated by the importance in improving the quality of III–V heteroepitaxy [1–3] and interest in surfactant-mediated epitaxy, surface passivation and delta-doping layers [4–7].

Previous experimental investigations of Sb adsorption on Si(0 0 1) have applied a variety of techniques such as low-energy electron diffraction (LEED) [8, 9, 10, 11], reflection high-energy electron diffraction (RHEED) [12, 13], core level spectroscopy [12, 13], scanning tunneling microscopy (STM) [8, 9, 13], surface extended X-ray absorption fine structure (SEXAFS) [8], medium energy ion scattering [11], transmission MeV ion channeling [10] and X-ray standing waves (XSW) [14]. In addition, the stability and structure have been calculated using the first principles molecular cluster approach (DMol) [15] and a total-energy calculation within the local-density approximation (LDA) [16]. It is generally accepted that Sb absorption at 400°C saturates at a coverage of nearly 1 monolayer (ML) (where 1 ML = 6.78×10^{14} atoms/cm^2 for Si(0 0 1)) with Sb atoms forming ad-dimers on top of nearly bulk-like Si. The well-known Si (2 × 1) dimer reconstruction has been removed, resulting in a Si(0 0 1)-Sb (1 × 2) symmetry. As the pentavalent Sb atoms can form three bonds (and one lone-pair orbital), and the tetravalent, top-layer Si atoms can form four bonds, there are no dangling bonds, and the surface is rather passive [5]. Unlike As, the saturation coverage of Sb is somewhat less than a full monolayer, ranging from 0.7 to 0.9 ML [11]. The breakup of the rows of dimers by defects and the high density of anti-phase domain boundaries imply a short coherence length for the domains of dimerized Sb. This explains the diffuseness and weakness of the half-order spots observed with electron diffraction. Although these experiments and calculations provided their own pieces of information to the structure of the Si(0 0 1)/Sb-(1 × 2) surface, these results are quantitatively far from agreement. A thorough picture of the Sb adsorption geometry on Si(0 0 1) has yet to be established.

* Corresponding author.

SSDI 0921-4526(95)00963-9

In this report, we present our recent XSW measurements on the saturated Si(0 0 1)/Sb-(1 × 2) surface. We have precisely measured the structure and bonding geometry for the Sb/Si(0 0 1) system. In addition, we have also directly measured the thermal vibrations of the Sb adatoms on the Si(0 0 1) surface in the [0 0 1] direction. This improves the uncertainty of the Sb dimer bond length measurement over our previous XSW measurement [14]. In combination with the results of the abovementioned SEXAFS measurement [8], we have experimentally determined the Si surface relaxation upon Sb adsorption. From the result of our experiment, we can also speculate about a possible anisotropy in thermal motion of the Sb adatoms.

2. XSW technique

Several years after its inception [17,18], the XSW technique was developed into a powerful probe for determining the precise lattice location of adatoms on single-crystal surfaces [19–22]. It combines the advantages of X-ray diffraction, interference and fluorescence spectroscopy. Unlike conventional diffraction techniques, which lose the phase information of the structure factor, the XSW method measures both the amplitude and the phase of the Fourier components. The XSW method is also element-specific, has high precision (typically 1% of the d-spacing) and does not require that the ad-layer structure have long-range order.

Based on the von Laue and Ewald theory for dynamical Bragg diffraction of an X-ray plane wave from a perfect single crystal (for a review, see Ref. [23]), the interference of the coherently coupled incident and Bragg-diffracted plane waves generates an XSW in Refs. [17,18], and above [19] the crystal, with the XSW nodal planes parallel to and having the same periodicity as the diffraction planes. The phase of the standing wave with respect to the diffraction planes shifts by 180° as the Bragg angle θ is scanned through the arc-second wide total reflection region of the Darwin curve. This inward sweep of the antinodal planes of the standing wave by one-half of the d-spacing (d_{hkl}), results in a modulation in the photoelectron, Auger, and fluorescent yields from any atoms residing within the interference field. Thus, it can be shown that the angular dependence of the normalized fluorescence yield $Y(\theta)$ from a spatial distribution of a specific atomic species near the surface can be described as

$$Y(\theta) = Y_{OB}\{1 + R(\theta) + 2\sqrt{R(\theta)}f_H \cos[v(\theta) - 2\pi P_H]\}, \quad (1)$$

where $R(\theta)$ is the reflectivity and $v(\theta)$ is the relative phase of the diffracted plane wave and Y_{OB} is the off-Bragg yield. The coherent fraction f_H and coherent position P_H correspond to the amplitude and phase, respectively, of the Hth Fourier component of the time-averaged spatial distribution of the nuclei of the adatoms (projected into a unit cell). $\boldsymbol{H}$ is the reciprocal lattice vector for the (hkl) diffraction planes. Let us consider the situation where N inequivalent ordered adsorption sites denoted by $\boldsymbol{r}_1, \boldsymbol{r}_2, \ldots, \boldsymbol{r}_N$ are occupied by a certain adatom species with occupation fractions of $C_1, C_2, \ldots, C_N$, respectively. Then the coherent position can be written as

$$P_H = \frac{1}{2\pi}\mathrm{Arg}\left[\sum_{n=1}^{N} C_n \exp(2\pi i \boldsymbol{H}\cdot\boldsymbol{r}_n)\right]. \quad (2)$$

In simple terms, P_H is a $\Delta d/d$ fractional position (mod 1). Based on the convolution theorem, the coherent fraction can be written as the product of three factors [21]:

$$f_H = C a_H D_H. \quad (3)$$

The ordered fraction $C = \sum_{n=1}^{N} C_n$ is the fraction of adatoms occupying ordered adsorption sites. The geometrical factor $a_H = 1/N|\sum_{n=1}^{N}(C_n/C)\exp(2\pi i \boldsymbol{H}\cdot\boldsymbol{r}_n)|$ accounts for multiple ordered sites. D_H is the Debye–Waller factor which accounts for the thermal vibration. This analysis is based on the dipole-approximation for photoelectric effect which makes the fluorescence yield from a certain adatom species proportional to the electric-field intensity at the center of the adatom.

For the case of Sb adsorption on Si(0 0 1), the Sb adatoms form symmetric (non-buckled) ad-dimers on Si(0 0 1) and have two equally occupied unit cell positions (see Fig. 1). Although there are (1 × 2) and (2 × 1) domains on the Si(0 0 1) surface due to single atomic steps in which ad-dimers are rotated 90° to each other, ad-dimers in these two domains give identical positions when projected along the [0 0 1] or [0 2 2] directions based on simple symmetry arguments. This is not true for the [1 1 1] direction and that is why we chose a [0 2 2] rather than a [1 1 1] XSW measurement to obtain in-plane structural information, i.e., ad-dimer bond length. Therefore, we used the (0 0 4) and (0 2 2) reflections and analyze the problem in terms of a one-domain (1 × 2) structure. For the (0 0 4) measurement, the coherent position is $P_{004} = h'/d_{004}$, where h' is the height of these adatoms above the Si(0 0 4) bulk-like lattice plane. Thermal vibrations smear the time-averaged spatial distribution of these adatoms. If individual atoms have a symmetrical time-averaged distribution about their mean position(s), the relation between the (0 0 8) and (0 0 4) coherent position is simply $P_{008} = h'/d_{008} = 2P_{004}$. If the ad-dimer is unbuckled (i.e., parallel to the Si(0 0 1) surface), the geometrical factors in the [0 0 1] direction are unity

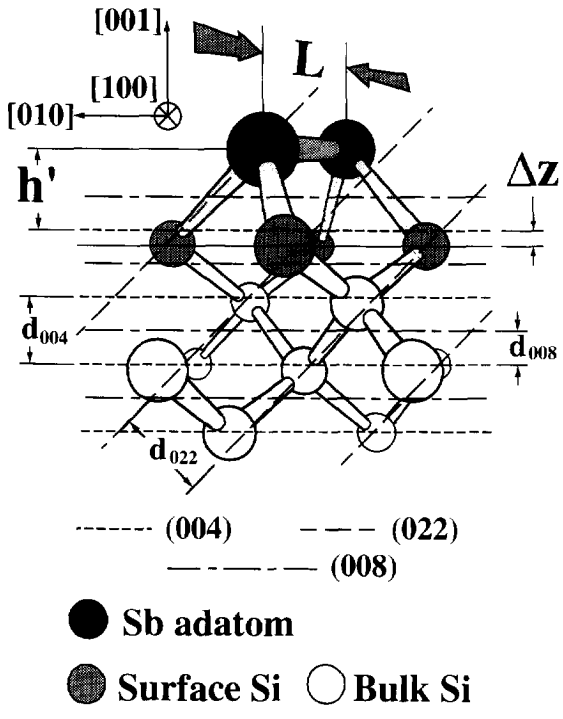

Fig. 1. A side view of the Si(001)/Sb-(1 × 2) surface ad-dimer model. The Si(004), (022) and (008) diffraction planes are represented by different sets of dashed lines. The solid line represents the height of the relaxed Si(001) surface. h' is the ad-dimer height above the bulk-like Si(001) surface atomic layer, Δz is the inward relaxation of the top Si layer, and L is the ad-dimer bond length. Note that the Sb ad-dimer bond does not lie in the plane of the figure.

($a_{004} = a_{008} = 1$). In the [022] direction the two adatom positions have inequivalent projections (Fig. 1), so that the geometrical factor $a_{022} = |\cos(\pi L/2d_{022})|$, where L is the ad-dimer bond length. Therefore, the ad-dimer bond length L can be determined as

$$L = \frac{2d_{022}}{\pi}\cos^{-1}\left[-\frac{f_{022}D_{004}}{f_{004}D_{022}}\right]. \tag{4}$$

The XSW experiment can also measure thermal vibrational amplitudes of adatoms relative to the bulk lattice by employing higher-order harmonic measurements [21,24]. The Debye–Waller factor can be expressed in terms of the adatom's thermal vibration amplitude $\sqrt{\langle u_H^2\rangle}$ as

$$D_H = \exp(-2\pi^2\langle u_H^2\rangle/d_H^2). \tag{5}$$

Based on Eqs. (3) and (5), if the ordered fraction (C) remains constant during the combined (004) and (008) XSW measurements, the thermal vibrational amplitude along the [001] direction can be determined from the measured (004) and (008) coherent fractions as

$$\sqrt{\langle u_H^2\rangle} = \frac{d_{004}}{\sqrt{6}\pi}\sqrt{\ln\frac{f_{004}}{f_{008}}}. \tag{6}$$

The (004)–(008) XSW combination also determines the ordered fraction (C) by the following equation:

$$C = \left[\frac{f_{004}^4}{f_{008}}\right]^{1/3}. \tag{7}$$

3. Experimental

The experiments were conducted at beamline X15A of the National Synchrotron Light Source (NSLS) at Brookhaven National Laboratory. The X15A ultrahigh vacuum (UHV) system (base pressure $\sim 9 \times 10^{-11}$ torr) consists of four coupled chambers allowing sample introduction, sample preparation (annealing, sputtering, MBE growth) and characterization (LEED, AES and XSW). The double-crystal monochromator at X15A produces a monochromated and collimated incident X-ray (Fig. 2). The X-ray beam is directed into the UHV chamber through a Be window and is Bragg reflected by the sample which is held by a UHV sample manipulator. The intensity of the Bragg-reflected X-ray beam was measured by an in vacuo Si photodiode. The X-ray fluorescence yield is recorded by an energy dispersive solid-state detector. In our experiments, a rocking curve about the (hkl) Bragg condition was accomplished by scanning the incident X-ray energy (using angular piezoelectric drives on both monochromator crystals). This is equivalent to scanning the angle of the sample substrate about the Bragg angle θ, and the abscissas of the data are therefore expressed as angular deflections. At each angular step, the reflected X-ray intensity and fluorescence spectrum were recorded simultaneously. The XSW technique as well as the experimental arrangement at X15A have recently been extensively reviewed by Zegenhagen [25].

To prepare a clean Si(001)-(2 × 1) surface, the sample was first Syton-polished and chemically cleaned ex situ using the Shiraki process [26]. It was mounted in a strain-free manner on a molybdenum holder and was introduced into the UHV system. After degassing the sample in UHV, the Shiraki oxide was thermally desorbed when the Si sample was flashed to 900°C for 10 min. The sample was then cooled to room temperature (initial cooling rate ≈ 2.0°C/s), resulting in a sharp, two-domain (2 × 1) LEED pattern. AES could detect no O and only a small amount of C contamination (~0.03 ML).

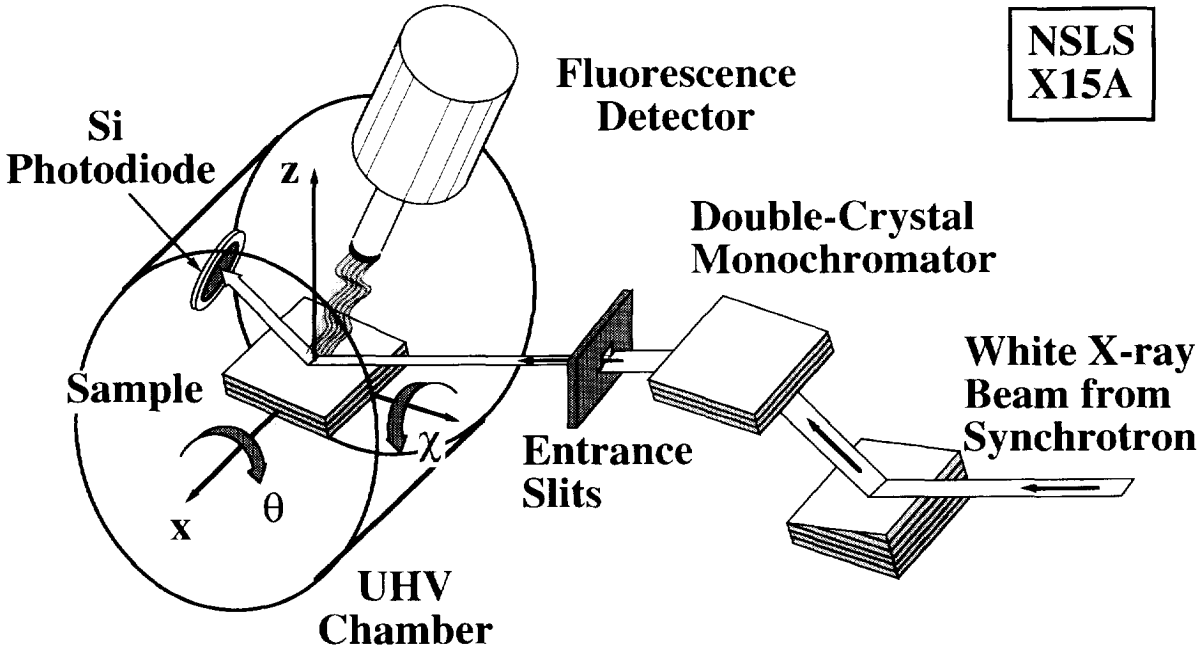

Fig. 2. A schematic drawing of the XSW experimental setup at X15A.

To prepare the saturated Si(0 0 1)/Sb-(1 × 2) surface, ≈3 ML of Sb was deposited from an effusion cell over 10 min with the Si substrate held at 550°C. Since the sticking coefficient for Sb adsorption goes to zero at coverages near 1 ML [11], approximately 1 ML Sb was adsorbed on the surface. The Sb-saturated surface was further annealed for 5 min at 550°C, resulting in a two domain (2 × 1) LEED pattern with slightly diffuse half-order spots.

On the saturated Si(0 0 1)/Sb-(1 × 2) surface, we performed XSW measurements using the Si (0 0 4), (0 2 2) and (0 0 8) Bragg reflections. We used 6.23 keV X-rays for the (0 0 4) measurement, 6.77 keV X-rays for the (0 2 2) measurement, and 9.60 keV for the (0 0 8) measurement (these energies are above the Sb L absorption edges). To do the (0 2 2) measurement, the sample had to be tilted 45° from the [0 0 1] direction (which is the surface normal) towards the [0 1 0] direction. To do the (0 0 8) measurement, an Al foil was placed between the monochromator and the sample to attenuate the coexisting 4.8 keV incident photons from the (0 0 4) reflection to less than 1%. To double check the stability of the surface, we then took another (0 0 4) XSW measurement immediately after the (0 0 8) measurement. The (0 0 4), (0 0 8) and (0 0 2) XSW results are shown in Fig. 3(a), (b) and (c), respectively.

4. Results and discussion

The coherent fractions (f_{004}, f_{022}, f_{008}) and coherent positions (P_{004}, P_{022}, P_{008}) shown in Fig. 3 (a) –(c) are determined by χ^2 fits of Eq. (1) to the Sb L fluorescence data. The measured value of $P_{004} = 1.21 \pm 0.01$ indicates that the Sb ad-dimer height $h' = P_{004} d_{004} = 1.64 \pm 0.02$ Å above the Si(0 0 4) bulk-like atomic planes. In a SEXAFS experiment, Richter et al. [8] measured the bond lengths for this surface system, finding a Sb–Si bond length of 2.63 ± 0.04 Å and a Sb–Sb bond length of 2.88 ± 0.03 Å. Assuming a symmetric dimer geometry, the SEXAFS values imply that the Sb ad-dimer resides 1.74 ± 0.05 Å above the surface Si plane. Therefore, we can combine the XSW and SEXAFS results to conclude that at room temperature the top layer Si atoms on the saturated Si(0 0 1)/Sb-(1 × 2) surface are relaxed inward by 0.10 ± 0.05 Å.

The Si surface relaxation for this surface system was also measured to be 0.09 ± 0.07 Å by an ion channeling method [10] and was predicted by the DMol calculation of Tang et al. [15] to be 0.05 ± 0.05 Å. the XSW–SEXAFS result is also consistent with the pseudo-potential calculation [27] of the relaxation of the As-terminated Si(0 0 1) surface (0.09 Å), which should exhibit a relaxation comparable to the present case.

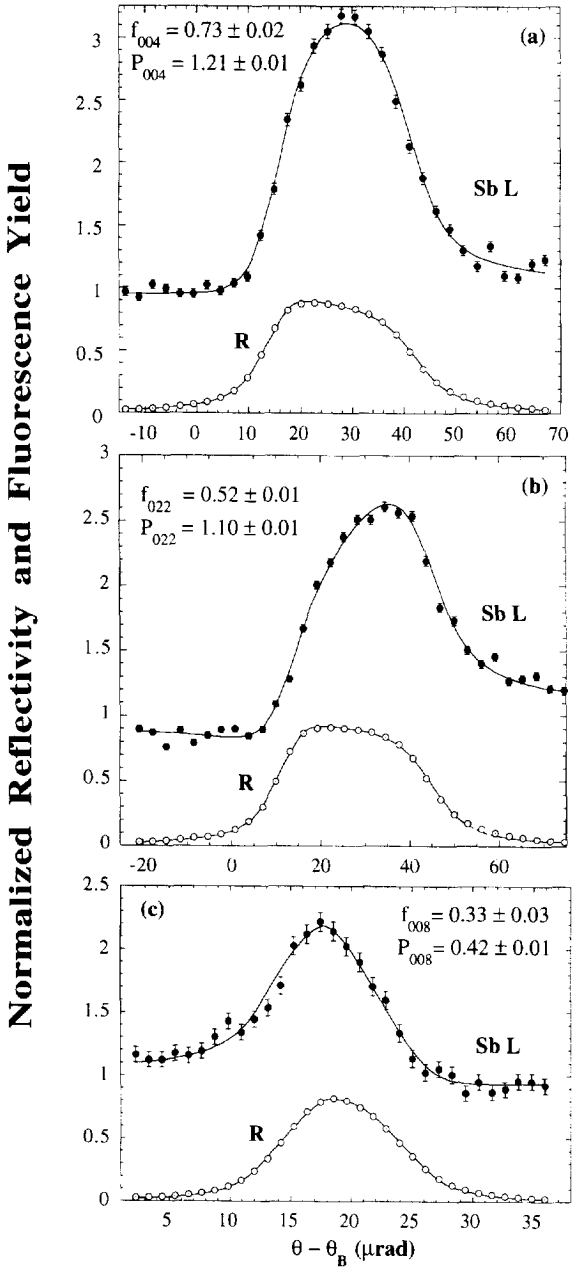

Fig. 3. Experimental data (dots) and theoretical curves (solid lines) for the normalized Sb L fluorescence yield and Si reflectivity (R) versus Bragg reflection angle θ for: (a) the Si(0 0 4) reflection, (b) the Si(0 2 2) reflection and (c) the Si(0 0 8) reflection from a saturated Si(0 0 1)/Sb-(1 × 2) surface.

As shown in Eq. (6), the thermal vibrational amplitude can be determined from f_{004} and f_{008} if the ordered fraction C is constant. We obtained the same f_{004} and P_{004} values for the (0 0 4) scans taken before and after the (0 0 8) measurement. This indicates that the surface structure and the ordering are very stable over a long period of time (~ 30 h) taken by the combined (0 0 4) and (0 0 8) measurements. With measured coherent fractions $f_{004} = 0.73 \pm 0.02$ and $f_{008} = 0.33 \pm 0.03$ and using Eq. (6), we found that the thermal vibrational amplitude of the Sb adatom in the [0 0 1] direction at room temperature is 0.156 ± 0.01 Å. From Eq. (7), the corresponding Sb ordered fraction was $C = 0.95$ for this surface preparation. This indicates that 95% of the Sb adsorbed on the Si surface is forming ad-dimers and the saturated Si(0 0 1)/Sb-(1 × 2) surface is highly ordered, similar to what has been found for other group V elements adsorption on Si(0 0 1) [28, 29].

We can compare our measured Sb $\sqrt{\langle u^2_{001}\rangle}$ value with other measured and calculated values of $\sqrt{\langle u^2_H\rangle}$ for the clean Si surface [30], and the As [28], Ga [24] and Bi [31] adsorbed Si surfaces (see Table 1).

To describe the geometry of symmetric Sb dimers, another piece of information that we need to specify is the Sb–Sb bond length L. As shown before, we can determine this quantity using Eqs. (3) and (4), if we know the Debye–Waller factor for the Sb adatoms along both [0 0 1] and [0 1 1] direction. In this experiment, we directly measured the Sb $\sqrt{\langle u^2_H\rangle}$ along the [0 0 1] direction. However, we do not have any direct measurement for the thermal vibration amplitude along the [0 1 1] direction. Therefore, we will start by assuming that the thermal vibration amplitude of Sb on the Si(0 0 1)/Sb-(1 × 2) surface at room temperature is isotropic. This is consistent with calculations for the clean Si(0 0 1) surface [32], and XSW measurements of the As/Si(0 0 1) surface [28]. Using our measured $\sqrt{\langle u^2_H\rangle}$ value, the Debye–Waller factors are $D_{004} = 0.77 \pm 0.03$ and $D_{022} = 0.88 \pm 0.02$. Eq. (4) then leads directly to a value of the Sb– Sb bond length of $L = 2.75 \pm 0.06$ Å.

In Table 2, we compare the structural parameters derived in this study under the assumption of symmetric dimers with previous theoretical and experimental studies of this surface system. Both experiments and calculations agree with each other on the Sb ad-dimer height and the top Si layer relaxation but disagree on the Sb dimer bond length. Our measured Sb dimer bond length value is in good agreement with that determined by ion channeling [10] and is also consistent with the Sb–Sb covalent bond length of 2.72 Å. Our value for the bond length L, however, is shorter than the value measured by SEXAFS [8], computed by the DMol calculation [15] and LDA calculation [16].

The above calculation of the Sb dimer bond length from the XSW measured values is based on the structural model which assumes that the Sb dimers are centered with respect to the underlying substrate and parallel to the surface. However, it was recently reported that on the

Table 1
Measured and calculated thermal vibration amplitudes $\sqrt{\langle u_H^2 \rangle}$ at room temperature

	Bulk Si[a]	Si on Si(1 1 1)[b]	Si on Si(0 0 1)[c]	Sb on Si(0 0 1)	As on Si(0 0 1)[d]	Ga on Si(0 0 1)[e]	Bi on Si(0 0 1)[f]
$\sqrt{\langle u_H^2 \rangle}$ (Å)	0.075	0.120	0.107	0.156	0.14	0.135	0.130

[a]Ref. [34].
[b,c]Ref. [30].
[d]Ref. [28].
[e]Ref. [24].
[f]Ref. [31].

Table 2
Theoretical and experimental values of structural dimensions for the saturated Si(0 0 1)/Sb-(1 × 2)surface. L is the Sb ad-dimer bond length. h and h' are the height of the Sb ad-dimer relative to the relaxed and unrelaxed Si(0 0 1) surface atomic planes, respectively. Δz represents the inward relaxation of the top layer Si(0 0 1) atoms. See Fig. 1

	Theory		Experiment		
	DMol[a]	LDA[b]	Ion Chanl.[c]	SEXAFS[d]	Present XSW
L (Å)	2.93 ± 0.05	2.96	2.8 ± 0.1	2.88 ± 0.03	2.75 ± 0.06
h (Å)	1.73	1.70		1.74 ± 0.05	
h' (Å)	1.68		1.63 ± 0.07		1.64 ± 0.02
$\Delta z = h - h'$ (Å)	0.05 ± 0.05		0.09 ± 0.07	0.10 ± 0.05	

[a]Ref. [15].
[b]Ref. [16].
[c]Ref. [10].
[d]Ref. [8].

Ge(0 0 1)/Sb-(1 × 2) surface the mid-point of the Sb dimer was shifted along the bond direction by 0.16 Å [33]. Our value of bond length of $L = 2.75 \pm 0.06$ Å has been calculated assuming no such shift. Additional Fourier components (e.g. (0 4 4) and (0 6 6)) are needed to uniquely determine whether the Sb ad-dimer is laterally shifted or not. Although it is not possible for us to conclude on the basis of the present data alone, we favor the symmetric-dimers model (i.e., no shift), based on its simplicity and on chemical bonding considerations.

The discrepancy between our XSW measured Sb–Sb bond length and results from SEXAFS measurement and calculations does not fall into the range of the experimental uncertainty. In our study, the Sb dimer bond length is determined from the f_{022} measured value by assuming that the Sb thermal vibration is isotropic. However, if we assumed that the Sb bond length was 2.88 ±0.04 Å as measured by SEXAFS, the f_{022} XSW value would imply an Sb thermal vibration amplitude of 0.22 ± 0.04 Å along the [0 1 1] direction at room temperature. Whether, or not, there exists such a large anisotropy for the Sb thermal motion at RT will be the focus of future and off-normal higher-order harmonic XSW measurements (e.g. using Si(0 4 4) and (0 6 6) reflections may resolve this issue).

5. Conclusions

We have measured the structure of Sb adsorption on the Si(0 0 1) surface using the XSW technique. We find that Sb atoms occur as symmetric dimers whose centers are located 1.64 ±0.02 Å above the bulk-like Si lattice plane with the Sb dimer bond length of 2.75 ±0.06 Å. Combined with previous SEXAFS measurements of the Sb–Si and Sb–Sb bond lengths, this implies an inward relaxation of the surface Si plane by 0.10 ±0.05 Å. Employing the higher-order harmonic measurement, the Sb room temperature thermal vibrational amplitude is determined experimentally to be 0.156 ±0.01 Å. Our measurements will be important in establishing a structural baseline for our upcoming experiments using Sb during surfactant mediated epitaxy, as well as for a stringent test of predictive theoretical calculations.

Acknowledgements

This work was supported by the US Department of Energy under contract No. W-31-109-ENG-38 to Argonne National Laboratory, contract No. DE-AC02-76CH00016 to National Synchrotron Light Source at Brookhaven National Laboratory, and by the National Science Foundation under contract No. DMR-9120521 to the MRC at Northwestern University. PFL is partially supported by National Institutes of Health under award No. IR01KD45295-01.

References

[1] D.K. Biegelsen, F.A. Ponce, A.J. Smith and J.C. Tramontana, J. Appl. Phys. 61 (1987) 1856.
[2] R.D. Bringans, M.A. Olmstead, R.I.G. Uhrberg and R.Z. Bachrach, Appl. Phys. Lett. 51 (1987) 523.
[3] H. Kroemer, J. Crystal Growth 81 (1987) 193.
[4] F.K. LeGoues, M. Copel and R. Tromp, Phys. Rev. Lett. 63 (1989) 1826.
[5] R.D. Bringans, D.K. Biegelsen, J.E. Northrup and L.E. Swark, Jpn. J. Appl. Phys. 32 (1993) 1484.
[6] D.J. Eaglesham, F.C. Unterwald and D.C. Jacobson, Phys. Rev. Lett. 70 (1993) 966.
[7] K. Sakamoto, K. Kyoya, K. Miki, H. Matsuhata and T. Sakamoto, Jpn. J. Appl. Phys. 32 (1993) L204.
[8] M. Richter, J.C. Woicik, J. Nogami, P. Pianetta, K.E. Miyano, A.A. Baski, T. Kendelewicz, C.E. Bouldin, W.E. Spicer, C.F. Quate and I. Lindau, Phys. Rev. Lett. 65 (1990) 3417.
[9] J. Nogami, A.A. Baski and C.F. Quate, Appl. Phys. Lett. 58 (1991) 475.
[10] M.W. Grant, P.F. Lyman, J.H. Hoogenraad and L.E. Seiberling, Surf. Sci. Lett. 279 (1992) L180 and private communication.
[11] W.F.J. Slijkerman, P.M. Zagwijn, J.F. van der Veen, D.J. Gravesteijn and G.F.A. van de Walle, Surf. Sci. 262 (1992) 25.
[12] D.H. Rich, T. Miller, G.E. Franklin and T.C. Chiang, Phys. Rev. B 39 (1989) 1438.
[13] D.H. Rich, F.M. Leibsle, A. Samsavar, E.S. Hirschorn, T. Miller and T.C. Chiang, Phys. Rev. B 39 (1989) 12758.
[14] P.F. Lyman, Y. Qian and M.J. Bedzyk, Surf. Sci. Lett. 325 (1995) L385.
[15] S. Tang and A.J. Freeman, Phys. Rev. B 47 (1993) 1460 and private communication.
[16] B.D. Yu and A. Oshiyama, Phys. Rev. B 50 (1994) 8942.
[17] B.W. Batterman, Phys. Rev. 133 (1964) A759.
[18] B.W. Batterman, Phys. Rev. Lett. 22 (1969) 703.
[19] P.L. Cowan, J.A. Golovchenko and M.F. Robbins, Phys. Rev. Lett. 44 (1980) 1680.
[20] J.A. Golovchenko, J.R. Patel, D.R. Kaplan, P.L. Cowan and M.J. Bedzyk, Phys. Rev. Lett. 49 (1982) 560.
[21] M.J. Bedzyk and G. Materlik, Phys. Rev. B 31 (1985) 4110.
[22] E. Fontes, J.R. Patel and F. Comin, Phys. Rev. Lett. 70 (1993) 2790.
[23] B.W. Batterman and H. Cole, Rev. Mod. Phys. 36 (1964) 681 and references therein.
[24] Y. Qian and M.J. Bedzyk, J. Vac. Sci. Technol. A 13 (1995) 1613.
[25] J. Zegenhagen, Surf. Sci. Rep. 18 (1993) 199.
[26] A. Ishizaka and Y. Shiraki, J. Electrochem. Soc. 133 (1986) 666.
[27] R.I.G. Uhrberg, R.D. Bringans, R.Z. Bachrach and J.E. Northrup, Phys. Rev. Lett. 56 (1986) 520.
[28] G.E. Franklin, E. Fontes, Y. Qian, M.J. Bedzyk, J.A. Golovchenko and J.R. Patel, Phys. Rev. B 50 (1994) 7483.
[29] G.E. Franklin, S. Tang, J.C. Woicik, M.J. Bedzyk, A.J. Freeman and J.A. Golovchenko, Phys. Rev. B., submitted
[30] O.L. Alerhand, J.D. Joannopoulos and E.J. Mele, Phys. Rev. B 39 (1989) 12622.
[31] P.F. Lyman, Y. Qian, T.L. Lee and M.J. Bedzyk, in preparation.
[32] A. Mazur and J. Pollmann, Surf. Sci. 225 (1990) 72.
[33] M. Lohmeier, H.A. van der Vegt, R.G. van Silfhout, E. Vlieg, J.M.C. Thornton, J.E. Macdonald and P.M.L.O. Scholte, Surf. Sci. 275 (1992) 190.
[34] K. Lonsdale, ed., International Tables for X-Ray Crystallography III (Kynoch, Birmingham, 1968).